Materials Science & Engineering A 631 (2015) 153–159

Contents lists available at ScienceDirect

Materials Science & Engineering A

journal homepage: www.elsevier.com/locate/msea

Effect of non-isothermal deformation of austenite on ferrite transformation behavior studied by in-situ neutron diffraction

Zengmin Shi [a,*], Yo Tomota [b], Stefanus Harjo [c], Yuhua Su [c], Bo Chi [d], Jian Pu [d], Li Jian [d,*]

[a] College of Materials and Chemical Engineering, China Three Gorges University, Yichang 443002, PR China
[b] Graduate School of Science and Engineering, Ibaraki University, 4-12-1 Nakanarusawa, Hitachi, Ibaraki 316-8511, Japan
[c] J-PARC Center, Japan Atomic Energy Agency, 2-4 Shirane Shirakata, Tokai, Ibaraki 319-1195, Japan
[d] School of Materials Science and Engineering, Huazhong University of Science and Technology, Wuhan 430074, PR China

ARTICLE INFO

Article history:
Received 20 November 2014
Received in revised form
16 February 2015
Accepted 16 February 2015
Available online 24 February 2015

Keywords:
Non-isothermal deformation
Neutron diffraction
Austenite
Ferrite
Steel

ABSTRACT

The microstructure evolution and phase transformation of high strength 22SiMn2TiB steel during non-isothermal deformation were investigated by using in situ time-of-flight (TOF) neutron diffraction technique. The results indicate that the deformation of austenite promotes pearlite and ferrite transformation while suppresses bainite transformation. Deformation texture forms in austenite and then it influences the evolution of transformation texture. Deformation of austenite brings the changes in lattice parameters of austenite caused by carbon partitioning and elastic strains during the transformation. Volume fraction of the retained austenite decreases with a decreased carbon content as deformation amount increases.

1. Introduction

In the non-isothermal mechanical process, deformation is accompanied simultaneously by the change of temperature and phase transformation; the plastic deformation of austenite caused by shape-forming is expected to have an effect on subsequent phase transformations and final microstructure. Deformation of metastable austenite is anticipated to increase the deformation stored energy in the deformed austenite and promotes the diffusional phase transformation. For ferrite transformation, austenite deformation enhances ferrite nucleation [1] and shortens the incubation period [2]. For bainite transformation, deformation of austenite has a two-fold effect; it raises bainite transformation start temperature B_s by increasing bainite nucleation, whereas retards bainite growth due to the hindrance of defects generated by the deformation, since bainite growth is orientation dependent [1,3–6]. Metastable austenite deformation promotes the diffusional phase transformation, which may result in carbon enrichment in the untransformed austenite. However, our previous studies indicated the austenite deformation increased the volume fraction of the retained austenite with the decreased carbon content during martensitic transformation [7]. The variant selection during phase transformation from the deformed parent austenite is still not clear, because of a sufficient quantity of austenite to investigate the deformation structure cannot be retained in practical low carbon and low alloyed steels.

In-situ neutron diffraction technique has been proved to be a powerful tool for various engineering applications due to the strong penetrability of neutron; it can obtain bulky averaged data, which enables to realize the microstructure evolution behaviors under different environmental conditions such as deformation, phase transformation and thermo-mechanical process [8–11]. Then in the present study, the steel 22SiMn2TiB was used to investigate the effect of non-isothermal compressive deformation of austenite on the subsequent transformation studied by in situ neutron diffraction technique. The effect of non-isothermal deformation in austenite on transformation and texture was explored.

2. Materials and experiments

Hot-rolled steel 22SiMn2TiB with a composition of Fe–0.22C–0.87Si–1.64Mn–0.024Ti–0.0015B–0.0025N (wt%) was used in this study. The microstructure of the as-received steel is martensite with a hardness value of 45.8 HRC. In situ neutron diffraction measurements were conducted using a TOF diffractometer, TAKUMI, at Material and Life Science Facility (MLF) in Japan Proton Accelerator Research Complex (J-PARC). The schematic illustration on the arrangement of the specimen with respect to the incident and diffracted neutron beams is presented in Fig. 1. The information from the axial

* Corresponding authors. Tel./fax: +86 717 6397505.
E-mail addresses: shzm@ctgu.edu.cn (Z. Shi), lijian@hust.edu.cn (L. Jian).

http://dx.doi.org/10.1016/j.msea.2015.02.043
0921-5093/

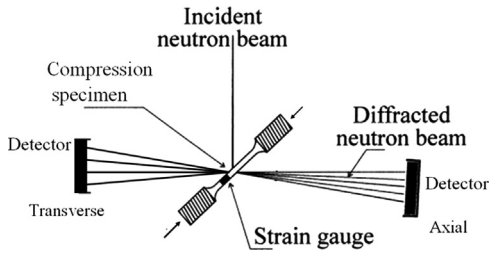

Fig. 1. Schematic illustration on the arrangement of in situ neutron diffraction.

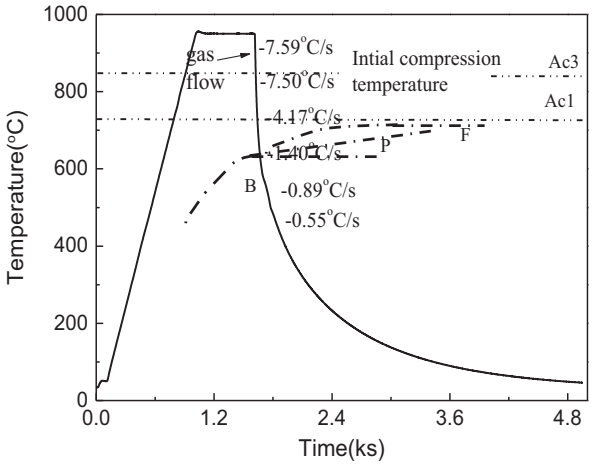

Fig. 2. Heating and cooling schedule of the specimen in neutron diffraction tests.

direction was obtained at the south detector while the transverse direction at the north detector. Cylinder specimens with a gauge dimension of $\varnothing 7 \times 14\ mm^2$ were heated up to austenitizing temperature 950 °C at a heating rate of 1 °C/s, then austenitized for 10 min followed by gas cooling above 850 °C, and finally cooled in gas atmosphere to room temperature. The acquisition period for each neutron spectrum was 60 s. It can be changed freely after the measurements because the data recording system at MLF/J-PARC is event mode. The measured cooling rate decreased with the decreasing of temperature, as shown in Fig. 2, and the cooling curve passes through the pearlite (P) and bainite (B) transformation region. During heating, the start and finish austenite transformation temperatures, Ac_1 and Ac_3, are 725 °C and 850 °C, respectively. During cooling, the specimens were continuously compressed starting from 850 °C and the compression finishing temperature was dependent on the amounts of deformation. The deformation amounts were 0%, 10% and 30% at a strain rate of $0.01\ s^{-1}$, implying that the specimen temperature was 850, 769 and 699 °C at the end of deformation, respectively.

The diffraction profiles in both the axial and transverse directions were collected simultaneously by the two separate detectors and analyzed by the Rietveld refinement method [12]. The volume fraction of austenite phase (v_γ) was correlated to the measured integrated intensities I^γ_{hkl} and I^α_{hkl} [13]

$$v_\gamma = \frac{(1/n)\sum^n (I^\gamma_{hkl}/R^\gamma_{hkl})}{((1/m)\sum^m (I^\alpha_{hkl}/R^\alpha_{hkl}) + (1/n)\sum^n (I^\gamma_{hkl}/R^\gamma_{hkl}))} \quad (1)$$

where (n) and (m) are the number of diffraction peaks for each constituent phase. R^α_{hkl} and R^γ_{hkl} are the theoretical integrated intensity of hkl-lattice spacing for ferrite matrix α and austenite γ with a random grain orientation distribution. The volume fraction of austenite was determined by using the integrated intensities of $(111)_\gamma$, $(200)_\gamma$, $(220)_\gamma$, $(311)_\gamma$, and that of ferrite $(110)_\alpha$, $(200)_\alpha$, $(211)_\alpha$ and $(310)_\alpha$ diffraction peaks. And the carbon content in the retained austenite was calculated according to the following equation [14]:

$$a_0 = 3.555 + 0.044C_\gamma \quad (2)$$

where a_0 is the lattice parameter of austenite in Å at room temperature, averagely estimated from the positions of $(111)_\gamma$, $(200)_\gamma$, $(220)_\gamma$ and $(311)_\gamma$ diffraction peaks, and C_γ is the carbon content in weight percentage. As will be explained later, the measured lattice constant at elevated temperatures were converted to that at room temperature by taking into account thermal expansion.

Gaussian function $G(\xi)$ is used to characterize the diffraction peaks by single peak fitting [8],

$$G(\xi) \sim \exp\left[-\frac{1}{2}\left(\frac{\xi - 2\pi/d}{\langle\beta^2\rangle^{1/2} 2\pi/d}\right)^2\right] \quad (3)$$

where ξ is the radial coordinate in the diffraction profiles, $\langle\beta^2\rangle^{1/2}$is the average microstrain in polycrystalline materials, $d$is the interplanar spacing. Lattice strain (ε) was determined by measuring the shift of diffraction peak position with temperature T as caused by the change in interplanar $d$spacing:

$$\varepsilon_{hkl} = (d^T_{hkl} - d^0_{hkl})/d^0_{hkl} \quad (4)$$

where, $d^T_{hkl}$is the interplanar d spacing at temperature T, $d^0_{hkl}$is the "reference". For austenite, the reference is the interplanar d spacing at austenite temperature 950 °C; while for ferrite, the reference is that of ferrite at room temperature.

The microstructure of the deformed specimen was examined by a Quanta 200A scanning electron microscope (SEM). EBSD images of the product phase were obtained by using an orientation imaging microscopy system attached to the Oxford X-Max SEM. The specimens for EBSD examination were mechanically polished. The step size for EBSD orientation mapping was 100 nm. The rolling (RD), transverse (TD), normal (ND) direction of the specimen were used for the standard coordinate system in the crystallographic orientation analysis. The compression direction corresponds to RD. The volume fractions of the product phases were determined by using the binary image segmentation procedures on the SEM microstructures.

3. Results and discussion

3.1. Microstructure features

Fig. 3 shows the SEM microstructures of the specimen non-isothermally deformed by 0%, 10% and 30%. As expected, bainite and pearlite colonies were observed in the non-deformed specimens as shown in Fig. 3(a), while polygonal-shaped ferrite (PF) was induced in the deformed specimens. The volume fraction of the polygonal-shaped ferrite increases from 0% to 31%, 50%,and that of pearlite colonies increases from 17% to 45%, 38%, with the increase of the deformation amount from 0% to 10% and 30%, respectively; while that of bainite is gradually depressed from 83% to 24% and 12%. It suggests that the deformation in austenite promotes pearlite and ferrite phase transformation rather than bainite. And it appears that the deformation accelerates the ferrite transformation a little faster than the pearlite transformation. The deformation in austenite also has a significant effect on the morphology of pearlite, as shown in Fig. 3(a′)–(c′). The deformation of 10% in austenite refines the pearlite lamellae, while the further increasing of deformation amount will coarsen the lamellae and compact the layer-meso-structure. Deformations in austenite caused deformation-induced ferrite phase transformation prior to pearlite and bainite transformation; the carbon partitioning between untransformed austenite and ferrite at elevated temperature was increased and then promoted pearlite transformation. At the same time, bainite transformation was retarded by the preferential ferrite formation and defects generated by deformation,